ISSN 0006-2979, Biochemistry (Moscow), 2024, Vol. 89, No. 7, pp. 1183-1191 © The Author(s) 2024. This article is an open access publication.

Use of qPCR to Evaluate Efficiency of the Bulky DNA Damage Removal in Extracts of Mammalian Cells with Different Maximum Lifespan

Aleksei A. Popov[1], Vladimir A. Shamanin[2], Irina O. Petruseva[1], Aleksei N. Evdokimov[1], and Olga I. Lavrik[1,3,a]*

[1]*Institute of Chemical Biology and Fundamental Medicine, Siberian Branch Russian Academy of Sciences, 630090 Novosibirsk, Russia*

[2]*LLC "BioLink", 630090 Novosibirsk, Russia*

[3]*Novosibirsk National Research State University, 630090 Novosibirsk, Russia*

[a]*e-mail: lavrik@niboch.nsc.ru*

Received March 1, 2024
Revised April 18, 2024
Accepted April 28, 2024

Abstract—Proteins of nucleotide excision repair system (NER) are responsible for detecting and removing a wide range of bulky DNA damages, thereby contributing significantly to the genome stability maintenance within mammalian cells. Evaluation of NER functional status in the cells is important for identifying pathological changes in the body and assessing effectiveness of chemotherapy. The following method, described herein, has been developed for better assessment of bulky DNA damages removal *in vitro*, based on qPCR. Using the developed method, NER activity was compared for the extracts of the cells from two mammals with different lifespans: a long-lived naked mole-rat (*Heterocephalus glaber*) and a short-lived mouse (*Mus musculus*). Proteins of the *H. glaber* cell extract have been shown to be 1.5 times more effective at removing bulky damage from the model DNA substrate than the proteins of the *M. musculus* cell extract. These results are consistent with the experimental data previously obtained. The presented method could be applied not only in fundamental studies of DNA repair in mammalian cells, but also in clinical practice.

DOI: 10.1134/S0006297924070022

Keywords: DNA repair, PCR, longevity

INTRODUCTION

DNA repair systems ensure maintenance of genome stability in the cells of a living organism, removal of the recurring damages induced by exogenous and endogenous factors, and repair the DNA structure [1]. Nucleotide excision repair (NER) proteins remove a wide range of bulky DNA lesions, including adducts formed by UV light and harmful polycyclic compounds from the environment. Such adducts cause significant disruptions in the regular double-stranded DNA structure, which are recognized by the XPC factor, which, in turn, induces recruitment of TFIIH and subsequent repair complex assembly at the damaged DNA region. After lesion verification by XPD helicase, excision of the DNA fragment containing bulky damage catalyzed by the XPF-ERCC1 and XPG endonucleases occurs. The resulting gap is filled in by synthesis using an intact DNA strand as a template and subsequent ligation; as a result, the original DNA structure is restored [1].

Since activity of the DNA repair systems determines resistance of the cells to genotoxic stress effects, functional status assessment of a particular DNA repair system in the cells is crucial in clinical practice

Abbreviations: BER, base excision repair; ODN, oligodeoxynucleotides; NER, nucleotide excision repair; nFlu, N-[6-(5(6)-fluoresceinylcarbamoyl)hexanoyl]-3-amino-1,2-propanediol; TEG, tetraethylene glycol.

* To whom correspondence should be addressed.

and is conducted to diagnose various pathological patterns. NER disruption is the cause of diseases such as Xeroderma pigmentosum and Cockayne syndrome, and decreased NER activity is expected to increase predisposition to cancer and premature aging [2-4]. At the same time, the increased NER activity characteristic of cancer cells could reduce effectiveness of a chemotherapy drug, since mechanism of their action is based on formation of bulky adducts in DNA [5-7].

In most NER studies, specific excision activity of the proteins was assessed by direct detection of the model DNA excision products or by post-excision radioactive labeling of the 3'-ends of these products [8-11]. A significant drawback of these methods, limiting their application in the clinic, is the necessity of using a radioactive label when constructing a model DNA, or detecting excision products. In this regard, quantitative polymerase chain reaction (qPCR) methods are of significant importance for the NER activity determination *in vitro*. The ability to assess the repair effectiveness by measuring fluorescence in combination with simple and fast implementation process makes qPCR-based methods promising tools for application not only for research purposes, but also in medicine. To date, two variants of the techniques for NER activity measurement involving the use of qPCR have been described. They are varying in complexity, architecture of model DNA, and type of bulky lesions to be removed (UV damage and DNA–protein crosslinking) [12, 13].

The goal of this work is development of a method for assessing effectiveness of elimination of bulky damage *in vitro* using qPCR and one of the damages effectively recognized and processed by NER proteins – polycyclic bulky damage analogue [8, 10, 14]. The developed approach was used to compare performance of the NER system in the cells of mammals with different lifespans, a long-lived naked mole-rat (*Heterocephalus glaber*) and a short-lived mouse (*Mus musculus*). The results show that the proteins in *H. glaber* cells more effectively remove bulky DNA lesions; this is consistent with the previously published data obtained by post-excision labeling [14].

MATERIALS AND METHODS

Preparation of DNA substrates. Sequences of oligodeoxynucleotides (ODNs) used to synthesize DNA substrates are shown in Table 1.

Table 1. Oligodeoxynucleotide and primer sequences used in the study

Name	Sequences
Oligodeoxynucleotides	
ODN-1	cgatgaagctggtggtcaactggtcctccatgaagcgggtccaagtcggcagtaccggcataacc
ODN-2-nFlu	aagcctatgcctacagcatccaggg(**nFlu**)gacggtgccgaggatgacgatgagcgca
ODN-2	aagcctatgcctacagcatccagggcgacggtgccgaggatgacgatgagcgca
ODN-3	ttgttagatttcatacacggtgatgctacaagttcgtggcg
ODN-4	gtaggcataggcttggttatgccggtactg
ODN-5	gtatgaaatctaacaatgcgctcatcgtcatcctcg
ODN-6	cgccacgaacttgtagcatcaccgtgtatgaaatctaacaa
ODN-7	tgcgctcatcgtcatcctcggcaccgtcgccctggatgctgtaggcataggctt
ODN-8	ggttatgccggtactgccgacttggacccgcttcatggaggacc(**PS-TEG**)gttgaccaccagcttcatcg
ODN-9	gacgatgagcgcattgttagatttcatacacgg
ODN-10	taccggcataaccaagcctatgcctaca
ODN-11	agctgctgctcatctcgagatctgagtacattggattgccattctccgagtgtattaccgtgacg
Primers	
Primer 1	cgccacgaacttgtagcatc
Primer 2	cgatgaagctggtggtcaa

Note. ODN, oligodeoxynucleotide sequence. Bold: nFlu, N-[6-(5(6)-fluoresceinylcarbamoyl)hexanoyl]-3-amino-1,2-propanediol; PS-TEG, tetraethylene glycol with a phosphothioate group introduced from the 5'-side.

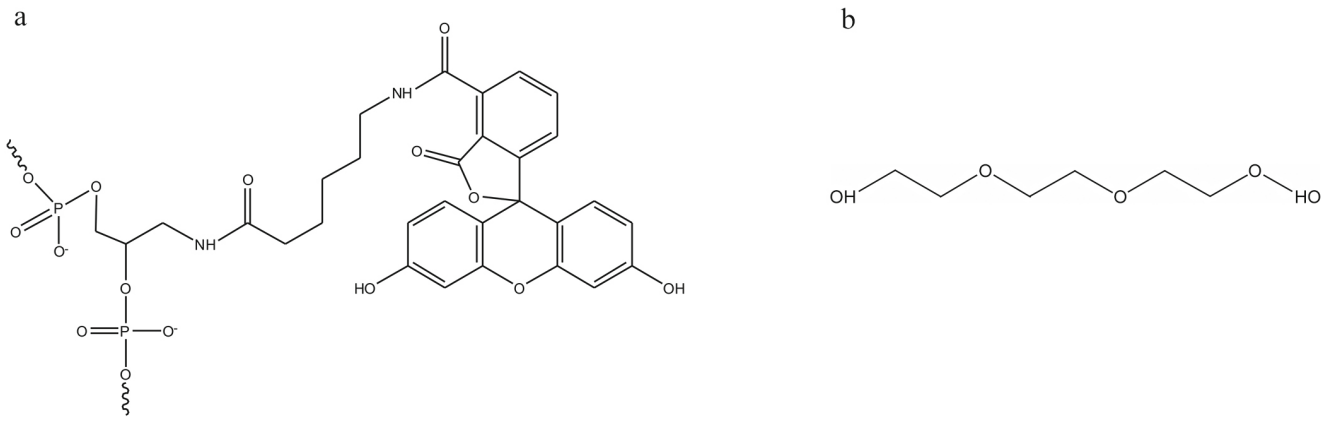

Fig. 1. Chemical structures of nFlu (a) and TEG (b).

To obtain a DNA strand with non-nucleotide modification of N-[6-(5(6)-fluoresceinylcarbamoyl) hexanoyl]-3-amino-1,2-propanediol (nFlu), ODN-1, ODN-2-nFlu, ODN-3, ODN-4, and ODN-5 were mixed in an equimolar ratio, then incubated at 95°C for 5 min and slowly cooled to room temperature. A ligation reaction mixture, which contained a mixture of hybridized ODN (10 μM), T4 DNA ligase (2 U/μl; SibEnzyme, Russia), ATP (10 mM), and 1 × DNA ligase T4 buffer (50 mM Tris-HCl (pH 7.5); 10 mM $MgCl_2$; 10 mM DTT; 1 mM ATP) was incubated for 16-18 h at 12°C. The reaction was stopped by incubation for 20 min at 70°C. The ligation reaction products were separated using 10% PAGE under denaturing conditions, and the target single-stranded (ss) DNA was isolated from the gel by electrotransfer to DEAE paper (Whatman, UK). Elution of the target ssDNA from the DEAE paper was carried out at 70°C by four portions (30 μl) of 3 M aqueous $LiClO_4$ solution; next DNA was precipitated with a 5-fold excess of cold acetone and incubated for 30-40 min at –20°C. After centrifugation (10 min, 12,000*g*, 4°C), the supernatant was removed and the pellet washed with cold acetone. The precipitate was then dried at room temperature and dissolved in H_2O.

Similar procedures were performed for synthesis of a non-modified strain (ODN-1, ODN-2, ODN-3, ODN-4, and ODN-5 were used) and a complementary strain of DNA containing modification on the basis of tetraethylene glycol (TEG) (ODN-6, ODN-7, ODN-8, ODN-9, and ODN-10 were used). Concentration of the obtained ssDNA was determined by measuring absorbance of the solution at 260 nm using a U-0080D spectrophotometer (Hitachi High-Technologies, Japan).

To form model DNA duplexes, nFlu- and TEG-containing strands (nFlu/TEG-DNA), as well as non-modified and TEG-containing strands (nm/TEG-DNA) were mixed in an equimolar ratio, after which they were incubated at 95°C for 5 min and cooled slowly to room temperature. Chemical structures of nFlu and TEG are shown in Fig. 1.

Cultivation of the cells. Naked mole-rat (NSF8) skin fibroblasts were cultured in a αMEM medium containing fetal calf serum (15% v/v; Thermo Fisher Scientific, USA), 10% AmnioMAX II Complete Medium (Thermo Fisher Scientific, basic fibroblast growth factor (bFGF; 5 ng/ml; PanEco, Russia), penicillin (0.1 U/ml), streptomycin (100 μg/ml), and amphotericin B (2.5 μg/ml), at 32°C under 5% CO_2 atmosphere. Mouse embryonic fibroblasts were cultured in a αMEM medium containing fetal calf serum (15% v/v;), penicillin (0.1 U/ml), streptomycin (100 μg/ml), and amphotericin B (2.5 μg/ml) at 37°C under 5% CO_2. All cell lines were provided by the IMCB SB RAS (General Biological Cell Culture Collection; no. 0310-2016-0002).

Preparation of NER-competent cell extracts. The work was carried out according to the protocol described by Reardon and Sancar [15]. Cells were resuspended in four PCVs (packed cell volume, volume of cells biomass pre-harvested by centrifugation for 10 min at 1000*g*) of hypotonic lysis buffer (10 mM Tris-HCl (pH 8.0); 1 mM EDTA; 5 mM DTT) and incubated for 20 min on ice, followed by destruction with a tight-fitting glass Potter homogenizer (20 pestle movements). The resulting homogenate in a glass beaker placed in an ice bath was resuspended in 4 PCV of sucrose-glycerol buffer [50 mM Tris-HCl (pH 8.0); 10 mM $MgCl_2$; 2 mM DTT; 25% (m/v) sucrose; 50% (v/v) glycerol], after which 1 PCV of a saturated neutralized solution of $(NH_4)_2SO_4$ (pH 7.0) was gradually added for over 30 min.

After ultracentrifugation (3 h, 100,000*g*, 4°C), the supernatant was collected and next finely ground $(NH_4)_2SO_4$ powder (at a ratio 0.33 g/ml) and 1 M NaOH were added thereto to maintain neutral pH. The resulted solution was stirred for 30 min. The pellet was collected by centrifugation (45 min, 12,000*g*, 4°C), followed by dissolution in an equal volume of buffer for NER-competent extracts (25 mM Hepes (pH 7.9); 100 mM KCl; 12 mM $MgCl_2$; 0.5 mM EDTA; 2 mM DTT; 12% (v/v) glycerol). The resulting solution

was dialyzed at 4°C against 500 ml of the same buffer for 2 h, after which the dialysis buffer was replaced with the freshly prepared one and dialysis was carried out for another 14-16 h. A precipitate of denatured protein was removed by centrifugation (10 min, 13,400*g*, 4°C). Aliquots of the resulting cell extract were frozen in liquid nitrogen and stored at –70°C.

Determination of protein concentration in cell extracts. Protein concentration in the extract preparations was determined with the Quick Start™ Bradford protein assay kit (Bio-Rad Laboratories, USA) following the provided instructions. BSA was used as a standard for calibration curve.

Conducting NER reaction. Reaction mixture for the NER reaction (30 μl), which contained 16 nM DNA substrate, 0.4 μg/μl NER competent cell extract, 0.5 mM deoxynucleoside triphosphate (dNTP) mixture, 0.066 U/μl Taq DNA polymerase and 0.5 μM oligodeoxynucleotide (ODN-11) for protection against nucleases specific for ssDNA regions (Table 1), in buffer (25 mM Tris-HCl (pH 7.8); 45 mM NaCl; 4.4 mM $MgCl_2$; 0.1 mM EDTA; 4 mM ATP) was incubated at 30°C for 30 min. The reaction was stopped by heating the reaction mixture at 65°C for 20 min. An aliquot of the reaction mixture inactivated after incubation with the extract proteins (1 μl) was diluted in H_2O (to DNA concentration of 1×10^{-12} M) and used for RT-qPCR analysis.

qPCR analysis. PCR reaction mixture (25 μl) contained 1 μl of diluted inactivated NER reaction mixture and the following components (final concentrations indicated): 0.3 μM primers 1 and 2 (Table 1); 0.06 U/μl Taq DNA polymerases with hot start; 0.25 mM dNTP mixture; 0.5×SYBR Green I dye (Lumiprobe, Russia); 1×PCR buffer (75 mM Tris-HCl (pH 8.8); 2 mM $(NH_4)_2SO_4$, 0.01% Tween 20; 3 mM $MgCl_2$). The reaction was carried out in 96-well plates (white, low-profile plastic; BIOplastics BV, Netherlands) in a LightCycler 96 amplifier (Roche, Switzerland) using the following PCR program: 95°C – 5 min, 1 cycle; 95°C – 15 s, 58°C – 15 s, 72°C – 10 s (detection of accumulated signal), 35 cycles; melting PCR products; cooling to 37°C.

Threshold cycle values, or C(t), obtained during the analysis of amplification curves were used to calculate the difference in dC(t) using the formula (1):

$$dC(t) = C(t)^{nFlu/TEG\text{-}DNA} - C(t)^{x}, \quad (1)$$

where $C(t)^{x}$ is the value of C(t) for the analyzed sample; $C(t)^{nFlu/TEG\text{-}DNA}$, C(t) value for nFlu/TEG-DNA in the control sample that was not exposed to cell extract proteins.

Statistical significance of the differences was determined using Student's *t*-test, * $p < 0.05$; ** $p < 0.01$; *** $p < 0.001$.

RESULTS AND DISCUSSION

We developed a qPCR-based method for assessing efficacy of the *in vitro* bulky lesion removal, which involves using an extended (160 bp) linear DNA duplex containing one modified link in each of the strands and NER-competent cell extracts as a substrate (Fig. 2).

Bulky modification of nFlu is easily recognized and removed from DNA by the proteins of the NER system [8, 10, 14]. The non-bulky modification based on TEG is an analogue of the apurine/apyrimidine site and is supposed to be subjected to the action of the proteins of the base excision repair (BER) system, however, the phosphothioate group, introduced from the 5′-side of TEG and resistant to nucleases [16], blocks the TEG processing by the endogenous AP endonuclease of extracts. Presence of these modifications in the strands of the DNA substrate prevents elongation of the primers 1 and 2 catalyzed by Taq DNA polymerase during PCR (Fig. 2). Removal of the DNA fragment containing nFlu by the proteins of the NER system should facilitate repair of one DNA strand, thereby this strand can be copied during elongation of the primer 1. This copy of DNA without modifications becomes a full-fledged template that is amplified during subsequent PCR cycles without difficulty.

During development of the method, we constructed and used two types of model DNA. The nFlu/TEG-DNA model contains both modifications and is a substrate for the NER system (Fig. 2). Relative position of nFlu and TEG in this DNA model ensures that the presence of TEG does not affect the ability of nFlu to undergo a specific excision reaction catalyzed by NER proteins [11]. The nm/TEG-DNA model containing only TEG simulates the repair product of the DNA substrate strand containing bulky damage (Fig. 2).

Using the synthesized templates and SYBR Green I as a fluorescent dye, PCR was performed to evaluate amplification conditions. PCR efficiency was calculated based on the calibration curve data, for which nm/TEG-DNA was used in the concentration range from 4×10^{-11} to 4×10^{-15} M (Fig. 3, a-c).

To evaluate amplification of the model nFlu/TEG-DNA and nm/TEG-DNA, we chose DNA concentration of 4×10^{-12} M. The results of comparative evaluation of the nFlu/TEG-DNA and nm/TEG-DNA amplification confirmed the possibility of using the DNA substrate designed in this study (Fig. 3g). Threshold cycle values C(t) for the nm/TEG and nFlu/TEG-DNA were 12.12 ± 0.29 and 19.28 ± 0.52 cycles, respectively (Fig. 3e); difference in the threshold cycle values between the nFlu/TEG- and nm/TEG-DNA (dC(t)) was 7.17 ± 0.43 cycles. Thus, the substrate and specific excision reaction product are distinguishable during PCR.

One possible reason for amplification of the nFlu/TEG-DNA may be presence in the synthesized

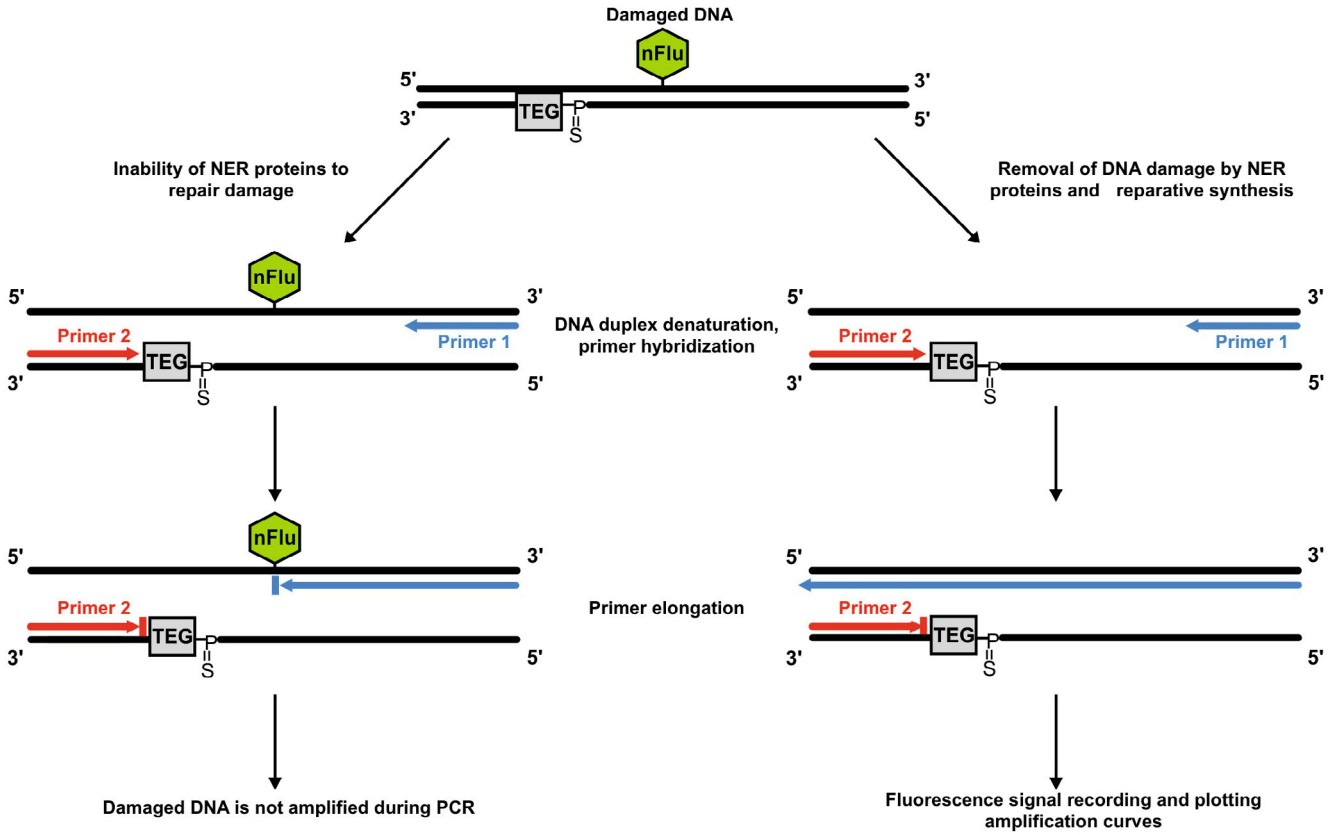

Fig. 2. Schematic representation of the proposed approach for evaluating removal of bulky lesions *in vitro* by qPCR.

preparation of an admixture of DNA containing a strand without modification (nm/TEG-DNA). Nevertheless, when analyzing melting curves of the nFlu/TEG-DNA and nm/TEG-DNA amplification products, we observed difference in the peaks of the PCR product melting curves and, as a result, revealed a slight difference in their melting points (Tm) – 90.37 ± 0.11°C for the nFlu/TEG-DNA and 90.99 ± 0.03°C for the nm/TEG-DNA, respectively (Fig. 3e). It could be suggested based on these data that the nucleotide sequences of the nFlu/TEG-DNA and nm/TEG-DNA amplification products are slightly different. It may be caused by the tendency of Taq DNA polymerase to translesion synthesis, when the enzyme could insert (although with low probability) a random nucleotide in the strand (preferably deoxyadenosine) opposite to the bulky DNA modification during the elongation stage [17-20].

Using the designed nFlu/TEG-DNA substrate, we evaluated efficiency of the *in vitro* removal of bulky DNA damage using proteins from the cells of long-lived naked mole-rat (*H. glaber*) and short-lived mouse (*M. musculus*) with the help of qPCR. To date, *H. glaber* cells are known to show high resistance to genotoxic effects, oncotransformation, and cellular aging, which is largely ensured by the effective functioning of cellular systems for maintaining genome stability [21-24]. Comparative assessment of the NER activity in *H. glaber* and *M. musculus* cells was previously carried out using the method of post-excision labeling of specific excision products [14]. The results of control experiments conducted in this study showed that efficiency of excision of the damaged DNA fragment containing nFlu from the model DNA duplex (137 bp) by the *H. glaber* cell extract proteins was 1.5-2 times higher compared to the efficiency exhibited by the proteins from *M. musculus* cells [14]. In this study we intended to compare the results obtained with the developed method with the data reported in our previous study by Evdokimov et al. [14]. For this purpose, similar preparations of *H. glaber* and *M. musculus* cell extracts were used as model systems. We also made some changes to adapt the NER response protocol to subsequent qPCR detection.

For PCR, not only the stage of specific excision of bulky damage is critical, but also the stage of the native strand structure repair (Fig. 2). Being model systems for *in vitro* determination of NER activity, the extracts of NER-competent cell derived from the cells or tissues of various types may differ in the content of components necessary for filling a single-strand gap. This fact may affect significantly the results of assessment of the NER excision activity using cell extracts. To offset these effects, we added Taq DNA polymerase and dNTP mixture to the reaction mixture for conducting NER.

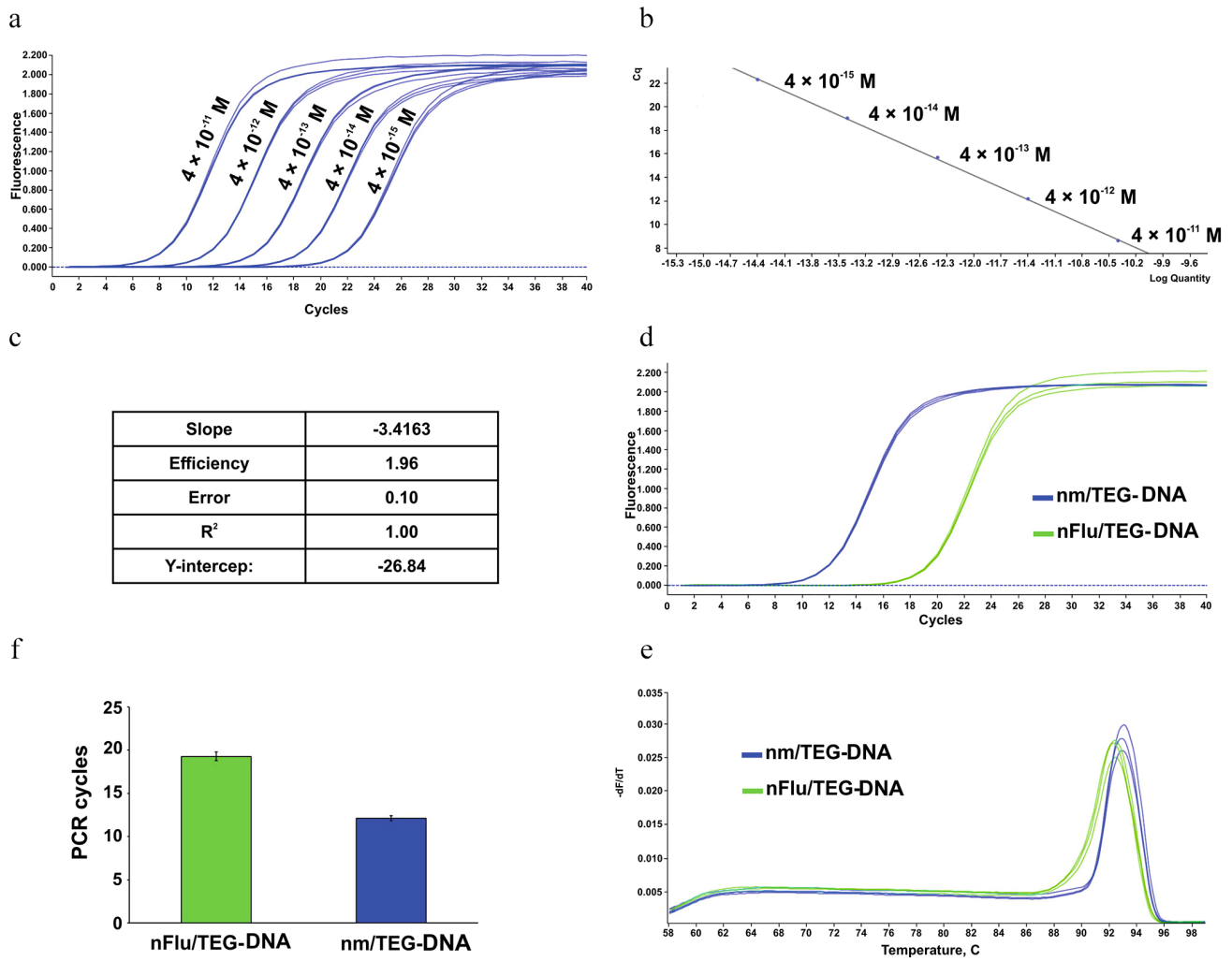

Fig. 3. Analysis of nFlu/TEG and nm/TEG DNA amplification results. Standard amplification curves for nm/TEG-DNA (a), calibration plot (b), and results of calculation of the nm/TEG-DNA amplification efficiency (c) are presented. d) Example of nm/TEG and nFlu/TEG-DNA amplification curves; e) average C(t) values and standard deviation of nm/TEG and nFlu/TEG-DNA based on three measurements; f) melting curves of nm/TEG and nFlu/TEG-DNA.

Using the developed protocol, we compared dependencies of the nFlu/TEG-DNA repair efficiency on incubation time for the *H. glaber* and *M. musculus* cell extract proteins (Fig. 4, a and b).

Efficiency of the nFlu/TEG-DNA repair was calculated based on the obtained mean dC(t) values converted to percentages. When calculating, the difference in C(t) for nFlu/TEG and nm/TEG-DNA obtained in the control experiments conducted without incubation of the model DNA with the extract proteins was taken as 100%. The nFlu/TEG-DNA repair efficiency was higher over the entire incubation interval with the *H. glaber* cell extract proteins (Fig. 4c) and after 30 min was 55.67 ± 0.42%, while after incubation with the *M. musculus* cell extract proteins the repair efficiency was significantly lower and was 35.17 ± 1.42% (Fig. 4d). Incubation of the nm/TEG-DNA with the proteins of cell extract for 30 min did not lead to a noticeable change in C(t) values. This fact indicates absence of the significant effect of non-specific exposure to the cell extract proteins in both cases. The *H. glaber* cell extract proteins were almost 1.5-fold more effective at removing nFlu bulky damage from the model DNA substrate than the *M. musculus* cell extract proteins. These data are consistent with the results of control experiments performed earlier using similar cell extract preparations by post-excision labeling of excision products [14]. Similarity of the Tm values and peak positions of the amplification product melting curves, which we observed for the nFlu/TEG-DNA processed by the extract proteins and the control nm/TEG-DNA (90.98 ± 0.04°C and 91.00 ± 0.06°C, respectively), further confirms the fact of removal of the bulky damage from DNA and repair of its correct nucleotide sequence in the process (Fig. 4d).

Despite the fact that the skin fibroblasts of the long-lived *H. glaber* and embryonic fibroblasts of the

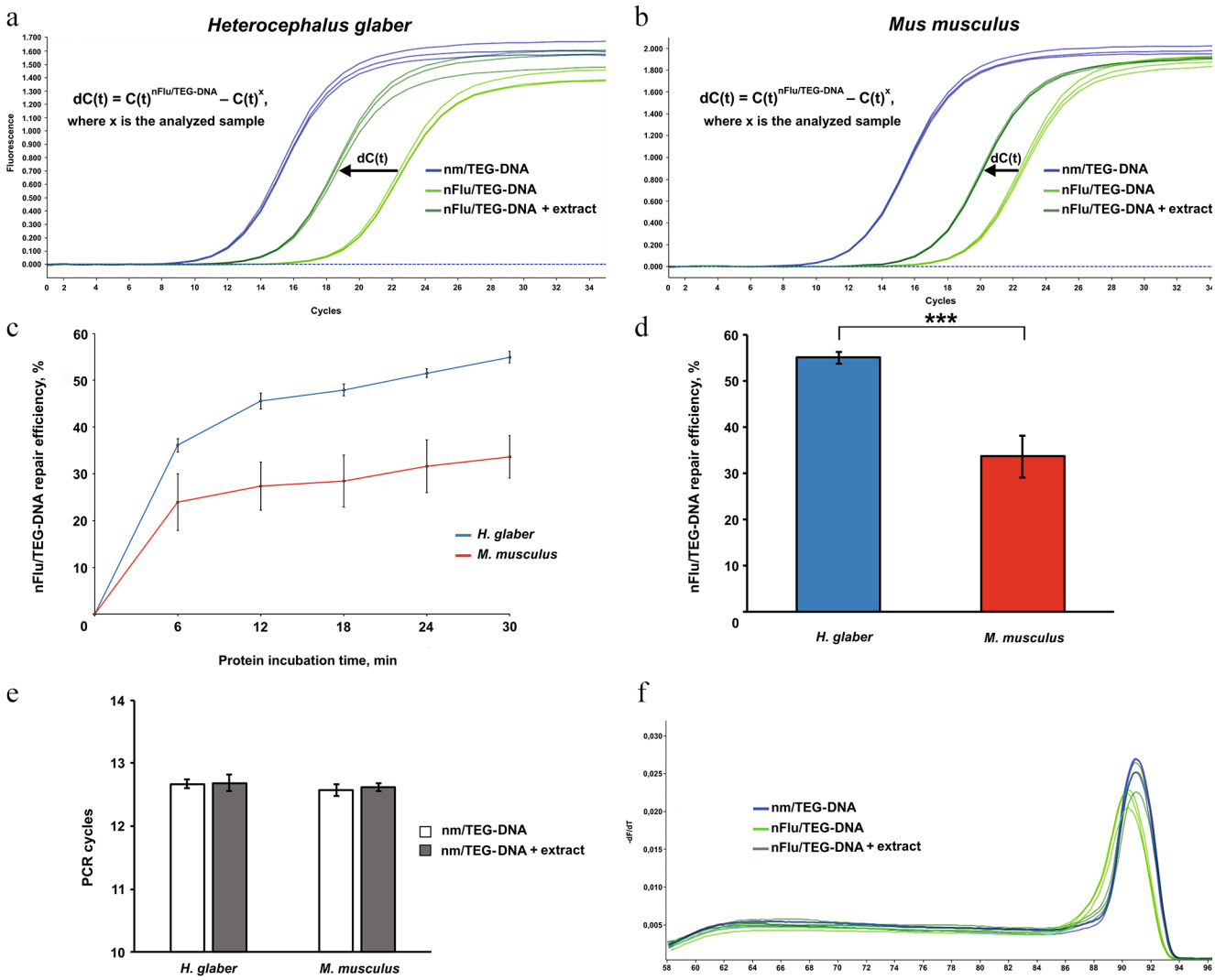

Fig. 4. Comparative evaluation of nFlu/TEG-DNA repair efficiency by *Heterocephalus glaber* and *Mus musculus* cell extract proteins with qPCR. nm/TEG-DNA amplification curves (violet), nFlu/TEG-DNA (green) and nFlu/TEG-DNA after 30 min incubation with extract proteins (dark green) obtained for *H. glaber* (a) and *M. musculus* (b); c) comparison of nFlu/TEG-DNA repair efficiency by NER proteins of *H. glaber* (blue) and *M. musculus* (red) cell extracts, depending on incubation time; d) difference in the nFlu/TEG DNA repair efficiency between *H. glaber* (blue) and *M. musculus* (red) cell extracts after 30 min of incubation; e) evaluation of the effect of *H. glaber* and *M. musculus* cell extract proteins on nm/TEG-DNA without bulky damage after 30 min incubation; f) example of melting curves showing nm/TEG-DNA (violet), nFlu/TEG-DNA (green), and nFlu/TEG-DNA amplification products after 30 min incubation with NER (dark green) proteins of *M. musculus* cell extract. Results are presented as a mean of three biological replicates with standard deviation, *** $p < 0.001$.

short-lived *M. musculus* used to test the developed method are different in nature, which may somewhat reduce the observed difference between the efficiency of bulky lesion removal by the proteins of these mammalian extracts, comparison of the results of post-excisional labeling with the qPCR results indicates that the removal of bulky damage by the NER system is indeed more effective in *H. glaber* cells. This is consistent with the current notions about the significant contribution of DNA repair systems in ensuring high genome stability of the *H. glaber*, which lives under constant oxidative stress [25-27]. Apparently, other DNA repair systems, such as BER, high activity of which was also noted in *H. glaber* cells, may play an important role in the effective removal of bulky damage in *H. glaber* cells [14, 27]. Possible participation of BER proteins, as well as some other systems in the repair of UV-induced damage has recently been demonstrated in the experiments with human cells deficient in XPA, one of the main protein factors involved in the NER process [28, 29]. Thus, the developed method is promising for further use in research aimed both at studying DNA repair in the cells of long-lived mammals and also at finding functional relationship of various DNA repair systems involved in the removal of bulky lesions.

CONCLUSION

The method we developed made it possible to evaluate efficiency of removing bulky DNA damage *in vitro* using extracts of the cells of long-lived *H. glaber* and short-lived *M. musculus*. Proteins of the *H. glaber* cell extract facilitated more effective recognition and removal of nFlu bulky damage from the model DNA substrate compared to the *M. musculus* cell extract proteins, which is consistent with the data published previously [14]. Hence, a simple and fast procedure for performing the developed method based on the use of qPCR analysis could promote its further widespread use both in basic research on the DNA repair processes and for timely assessment of the status of DNA repair systems of the patients in clinical practice.

Contributions. I.O.P. and O.I.L. supervised the study; A.A.P., V.A.Sh., and I.O.P. conducted experiments; A.A.P., I.O.P., A.N.E., and O.I.L. prepared and edited the manuscript.

Funding. This work was financially supported by the Russian Science Foundation (project no. 19-74-10056-P).

Ethics declaration. This work does not describe any studies involving humans or animals as objects performed by any of the authors. The authors of this work declare that they have no conflicts of interest.

REFERENCES

1. Chatterjee, N., and Walker, G. C. (2017) Mechanisms of DNA damage, repair, and mutagenesis, *Environ. Mol. Mutagen.*, **58**, 235-263, https://doi.org/10.1002/em.22087.
2. Krasikova, Y., Rechkunova, N., and Lavrik, O. (2021) Nucleotide excision repair: from molecular defects to neurological abnormalities, *Int. J. Mol. Sci.*, **22**, 6220, https://doi.org/10.3390/ijms22126220.
3. Paccosi, E., Balajee, A. S., and Proietti-De-Santis, L. (2022) A matter of delicate balance: loss and gain of Cockayne syndrome proteins in premature aging and cancer, *Front. Aging*, **3**, 960662, https://doi.org/10.3389/fragi.2022.960662.
4. Yurchenko, A. A., Rajabi, F., Braz-Petta, T., Fassihi, H., Lehmann, A., Nishigori, C., Wang, J., Padioleau, I., Gunbin, K., Panunzi, L., Morice-Picard, F., Laplante, P., Robert, C., Kannouche, P. L., Menck, C. F. M., Sarasin, A., and Nikolaev, S. I. (2023) Genomic mutation landscape of skin cancers from DNA repair-deficient xeroderma pigmentosum patients, *Nat. Commun.*, **14**, 2561, https://doi.org/10.1038/s41467-023-38311-0.
5. Kap, E. J., Popanda, O., and Chang-Claude, J. (2016) Nucleotide excision repair and response and survival to chemotherapy in colorectal cancer patients, *Pharmacogenomics*, **17**, 755-794, https://doi.org/10.2217/pgs-2015-0017.
6. Bowden, N. A. (2014) Nucleotide excision repair: why is it not used to predict response to platinum-based chemotherapy? *Cancer Lett.*, **346**, 163-171, https://doi.org/10.1016/j.canlet.2014.01.005.
7. Kiwerska, K., and Szyfter, K. (2019) DNA repair in cancer initiation, progression, and therapy-a double-edged sword, *J. Appl. Genet.*, **60**, 329-334, https://doi.org/10.1007/s13353-019-00516-9.
8. Evdokimov, A., Petruseva, I., Tsidulko, A., Koroleva, L., Serpokrylova, I., Silnikov, V., and Lavrik, O. (2013) New synthetic substrates of mammalian nucleotide excision repair system, *Nucleic Acids Res.*, **41**, e123, https://doi.org/10.1093/nar/gkt301.
9. Liu, Z., Ding, S., Kropachev, K., Lei, J., Amin, S., Broyde, S., and Geacintov, N. E. (2015) Resistance to nucleotide excision repair of bulky guanine adducts opposite abasic sites in DNA duplexes and relationships between structure and function, *PLoS One*, **10**, e0142068, https://doi.org/10.1371/journal.pone.0137124.
10. Lukyanchikova, N. V., Petruseva, I. O., Evdokimov, A. N., Silnikov, V. N., and Lavrik, O. I. (2016) DNA with damage in both strands as affinity probes and nucleotide excision repair substrates, *Biochemistry (Moscow)*, **81**, 263-274, https://doi.org/10.1134/S0006297916030093.
11. Naumenko, N., Petruseva, I., Lomzov, A., and Lavrik, O. (2021) Recognition and removal of clustered DNA lesions via nucleotide excision repair, *DNA Repair (Amst)*, **108**, 103225, https://doi.org/10.1016/j.dnarep.2021.103225.
12. Chesner, L. N., and Campbell, C. (2018) A quantitative PCR-based assay reveals that nucleotide excision repair plays a predominant role in the removal of DNA-protein crosslinks from plasmids transfected into mammalian cells, *DNA Repair (Amst)*, **62**, 18-27, https://doi.org/10.1016/j.dnarep.2018.01.004.
13. Shen, J. C., Fox, E. J., Ahn, E. H., and Loeb, L. A. (2014) A rapid assay for measuring nucleotide excision

repair by oligonucleotide retrieval, *Sci. Rep.*, **4**, 4894, https://doi.org/10.1038/srep04894.

14. Evdokimov, A., Kutuzov, M., Petruseva, I., Lukjanchikova, N., Kashina, E., Kolova, E., Zemerova, T., Romanenko, S., Perelman, P., Prokopov, D., Seluanov, A., Gorbunova, V., Graphodatsky, A., Trifonov, V., Khodyreva, S., and Lavrik, O. (2018) Naked mole rat cells display more efficient excision repair than mouse cells, *Aging (Albany NY)*, **10**, 1454-1473, https://doi.org/10.18632/aging.101482.
15. Reardon, J. T., and Sancar, A. (2006) Purification and characterization of *Escherichia coli* and human nucleotide excision repair enzyme systems, *Methods Enzymol.*, **408**, 189-213, https://doi.org/10.1016/S0076-6879(06)08012-8.
16. Clavé, G., Reverte, M., Vasseur, J. J., and Smietana, M. (2020) Modified internucleoside linkages for nuclease-resistant oligonucleotides, *RSC Chem. Biol.*, **2**, 94-150, https://doi.org/10.1039/d0cb00136h.
17. Smith, C. A., Baeten, J., and Taylor, J. S. (1998) The ability of a variety of polymerases to synthesize past site-specific cis-syn, trans-syn-II, (6-4), and Dewar photoproducts of thymidylyl-(3′→5′)-thymidine, *J. Biol. Chem.*, **273**, 21933-21940, https://doi.org/10.1074/jbc.273.34.21933.
18. Taylor, J. S. (2002) New structural and mechanistic insight into the A-rule and the instructional and non-instructional behavior of DNA photoproducts and other lesions, *Mutat. Res.*, **510**, 55-70, https://doi.org/10.1016/s0027-5107(02)00252-x.
19. Khare, V., and Eckert, K. A. (2002) The proofreading 3′→5′ exonuclease activity of DNA polymerases: a kinetic barrier to translesion DNA synthesis, *Mutat. Res.*, **510**, 45-54, https://doi.org/10.1016/s0027-5107(02)00251-8.
20. Obeid, S., Schnur, A., Gloeckner, C., Blatter, N., Welte, W., Diederichs, K., and Marx, A. (2011) Learning from directed evolution: *Thermus aquaticus* DNA polymerase mutants with translesion synthesis activity, *Chembiochem.*, **12**, 1574-1580, https://doi.org/10.1002/cbic.201000783.
21. Evdokimov, A., Popov, A., Ryabchikova, E., Koval, O., Romanenko, S., Trifonov, V., Petruseva, I., Lavrik, I., and Lavrik, O. (2021) Uncovering molecular mechanisms of regulated cell death in the naked mole rat, *Aging (Albany NY)*, **13**, 3239-3253, https://doi.org/10.18632/aging.202577.
22. Yamamura, Y., Kawamura, Y., Oka, K., and Miura, K. (2022) Carcinogenesis resistance in the longest-lived rodent, the naked mole-rat, *Cancer Sci.*, **113**, 4030-4036, https://doi.org/10.1111/cas.15570.
23. Boughey, H., Jurga, M., and El-Khamisy, S. F. (2021) DNA homeostasis and senescence: lessons from the naked mole rat, *Int. J. Mol. Sci.*, **22**, 6011, https://doi.org/10.3390/ijms22116011.
24. Hadj-Moussa, H., Eaton, L., Cheng, H., Pamenter, M. E., and Storey, K. B. (2022) Naked mole-rats resist the accumulation of hypoxia-induced oxidative damage, *Comp. Biochem. Physiol. A Mol. Integr. Physiol.*, **273**, 111282, https://doi.org/10.1016/j.cbpa.2022.111282.
25. Buffenstein, R. (2005) The naked mole-rat: a new long-living model for human aging research, *J. Gerontol. A Biol. Sci. Med. Sci.*, **60**, 1369-1377, https://doi.org/10.1093/gerona/60.11.1369.
26. Gorbunova, V., Seluanov, A., Zhang, Z., Gladyshev, V. N., and Vijg, J. (2014) Comparative genetics of longevity and cancer: insights from long-lived rodents, *Nat. Rev. Genet.*, **15**, 531-540, https://doi.org/10.1038/nrg3728.
27. MacRae, S. L., Croken, M. M., Calder, R. B., Aliper, A., Milholland, B., White, R. R., Zhavoronkov, A., Gladyshev, V. N., Seluanov, A., Gorbunova, V., Zhang, Z. D., and Vijg, J. (2015) DNA repair in species with extreme lifespan differences, *Aging (Albany NY)*, **7**, 1171-1184, https://doi.org/10.18632/aging.100866.
28. Gautam, A., Fawcett, H., Burdova, K., Brazina, J., and Caldecott, K. W. (2023) APE1-dependent base excision repair of DNA photodimers in human cells, *Mol. Cell*, **83**, 3669-3678.e7, https://doi.org/10.1016/j.molcel.2023.09.013.
29. Saha, L. K., Wakasugi, M., Akter, S., Prasad, R., Wilson, S. H., Shimizu, N., Sasanuma, H., Huang, S. N., Agama, K., Pommier, Y., Matsunaga, T., Hirota, K., Iwai, S., Nakazawa, Y., Ogi, T., and Takeda, S. (2020) Topoisomerase I-driven repair of UV-induced damage in NER-deficient cells, *Proc. Natl. Acad. Sci. USA*, **117**, 14412-14420, https://doi.org/10.1073/pnas.1920165117.